ELSEVIER

Biochimica et Biophysica Acta 1364 (1998) 73–83

BIOCHIMICA ET BIOPHYSICA ACTA
BBA

Isolation of mutants of the *Arabidopsis thaliana* alternative oxidase (ubiquinol:oxygen oxidoreductase) resistant to salicylhydroxamic acid

Deborah A. Berthold *

Department of Plant and Microbial Biology, 111 Koshland Hall, University of California, Berkeley, CA 94720-3102, USA

Received 24 October 1997; accepted 28 January 1998

Abstract

The plant-type ubiquinol:oxygen oxidoreductase, commonly called the alternative oxidase, is a respiratory enzyme thought to contain non-heme iron at its active site. To explore the structure of the enzyme by identifying amino acids involved in inhibitor-binding, a library of random mutants of the *Arabidopsis thaliana* alternative oxidase was constructed using error-prone polymerase chain reaction and expressed in the heme-deficient *Escherichia coli* SASX41B. Selection for resistance to salicylhydroxamic acid (SHAM) resulted in the recovery of four mutations. Three of these, F215L, M219I, and M219V, confer a small, but measurable resistance to SHAM of between 1.4- and 1.7-fold relative to the wild type alternative oxidase. These changes are located in a putative amphipathic helix following the second transmembrane helix. The fourth mutation, G303E, is found three residues from the C-terminus of the protein, and results in 4.6-fold resistance to SHAM. None of the mutations have any effect on the sensitivity of the alternative oxidase to propyl gallate. The identification of distant residues involved in SHAM resistance suggests that the poorly conserved C-terminal region is in spatial proximity to the amphipathic helix, and thus located in the vicinity of the iron-binding motif. © 1998 Elsevier Science B.V.

Keywords: Alternative oxidase; Plant-type ubiquinol:oxygen oxidoreductase; Plant mitochondrion; Salicylhydroxamic acid; Inhibitor-resistance; Cyanide-resistant respiration

1. Introduction

The alternative oxidase is a novel ubiquinol:oxygen oxidoreductase found in all plant and many algal and fungal mitochondrial respiratory chains, as well as in the bloodstream form of the parasitic protozoan, trypanosome [1,2]. Unlike cytochrome *c* oxidase, which also catalyzes the four-electron reduction of oxygen to water, the alternative oxidase does not translocate protons, allowing electron transfer to proceed without coupling to ATP synthesis. Using plant mitochondria the alternative oxidase has been shown to be activated by pyruvate and also by reduction of the disulfide bond that links the two identical subunits comprising the enzyme [3,4]. Hydropathy analysis of the deduced protein sequence from six plants, two fungi and a protozoan reveals two transmembrane helices connected by an intervening region of helical charac-

* Present address: Dept. of Plant Biology, University of Illinois, 265 Morrill Hall, 505 S. Goodwin Ave., Urbana, IL 61801, USA. E-mail: berthold@uiuc.edu

PII S0005-2728(98)00015-2

ter [5]. It is clear from spectroscopic studies of the partially purified enzyme that no heme or iron–sulfur center is present [6], although the appearance of enzyme activity requires iron, as shown in work with the fungus *Pichia anomala* [7]. A conserved sequence motif similar to the active site of the hydroxylase enzyme of methane monooxygenase suggests the presence of a binuclear iron center, and the lack of a visible absorption spectrum provides evidence for a μ-hydroxo-bridge linking the iron atoms [8]. Although work has been done identifying residues involved in the mitochondrial import of the alternative oxidase precursor [9] and the regulation of activity by covalent modification [10] there is yet no experimental evidence as to which residues may be involved at the active site of the enzyme.

One strategy for locating amino acids involved in quinone binding has been the isolation of mutants resistant to inhibitors that act as quinone analogs. The validity of this method rests upon the assumption that the mutated residues that bestow inhibitor-resistance are located at the quinone-binding site. For the case of the bacterial photosynthetic reaction centers, this assumption has been verified by high-resolution structures [11,12]. Through the use of inhibitor-resistant mutants, residues involved in quinone-binding in photosystem II [13] and the cytochrome bc_1 complex have been located [14]. In the current work, this strategy has been adopted for the study of the alternative oxidase.

To locate residues involved in the binding of the inhibitor salicylhydroxamic acid (SHAM), a potential substrate-analog, the ability of *Escherichia coli* to express a functional alternative oxidase was utilized [15]. The heme-deficient *E. coli* strain SASX41B is unable to grow aerobically owing to a defect in the gene for glutamyl-tRNA dehydrogenase in the 5-aminolevulinic acid (ALA) synthesis pathway [16]. This results in the absence of the endogenous terminal oxidases, cytochrome *bo* oxidase and cytochrome *bd* oxidase. Complementation of *E. coli* SASX41B with the *Arabidopsis thaliana* alternative oxidase permits aerobic growth [15]. In this study, a library of random mutants of the alternative oxidase was constructed and expressed in *E. coli* SASX41B, and SHAM-resistant mutants of the alternative oxidase were isolated.

2. Materials and methods

2.1. E. coli strains and growth media

E. coli strain DH5α was used for cloning and investigation of the effect of inhibitors on wild-type *E. coli* respiration. *E. coli* GO103 (*thi*, *gal*, *rpsL*, *zbg*::Kan, Δ(*cydAB*)455), which lacks the cytochrome *bd* oxidase, was used for investigation of alternative oxidase inhibitors on the cytochrome *bo* oxidase. *E. coli* SASX41B (*HfrP02A hemA41 metB1 relA1*), an ALA auxotroph [17], was used for expression of the alternative oxidase. *E. coli* GO103 was obtained from R. Gennis, Urbana, IL, and *E. coli* SASX41B from D. Söll, New Haven, CT.

For isolation of colonies, the strains were grown on either LB agar with 60 μg/ml ampicillin or GA agar (1.2% agar, 1% NaCl, 1% bactotryptone, 0.1% yeast extract, 0.3% disodium succinate hexahydrate, 0.3% DL sodium lactate, 5 mg/l $FeSO_4 \cdot 7H_20$, and 60 μg/ml ampicillin). For liquid culture, strains were grown in LB media or M63 + SG, (M63 [18] with 0.1 mM $CaCl_2$, 0.3% disodium succinate hexahydrate, 0.2% (v/v) glycerol, 0.1% yeast extract, 0.1% casamino acids, and 11.2 mg/l $FeSO_4 \cdot 7H_2O$ (total concentration), pH 7.2.) Solid and liquid media were supplemented with 50 μg/ml ALA, 60 μg/ml ampicillin, 40 μg/ml methionine, 1 μg/ml thiamin, and 0.3–0.6 mM salicylhydroxamic acid as required. *E. coli* GO103 was grown with 25 μg/ml kanamycin.

2.2. Construction of the mutant libraries

The plasmid pAOX, containing the gene for the *A. thaliana* alternative oxidase in the expression vector pcDNAII ([15], from M. Kumar and D. Söll, New Haven, CT), was modified to aid current and future cloning of mutagenized fragments of the alternative oxidase gene (Fig. 1). The *Xho*I site in the linker region was destroyed by digestion, filling in, and religation forming pAtAOmX. A single base change (A to T) within the *Kpn*I restriction site removed this site from the linker region, forming pAtAOmKX. This plasmid expressed the alternative oxidase in *E. coli* SASX41B at levels indistinguishable from pAOX.

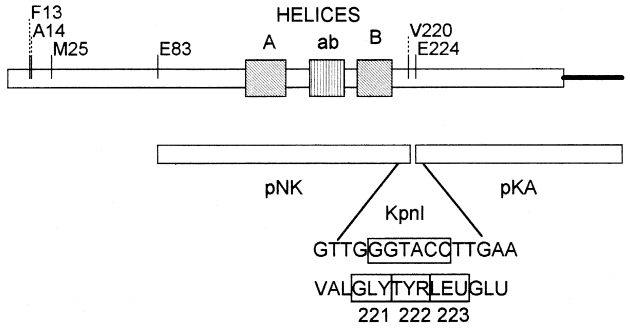

Fig. 1. The portion of the *Arabidopsis* alternative oxidase subject to random mutagenesis using the subcloned fragments pNK and pKA. The upper box depicts the amino-acid sequence of the *Arabidopsis* alternative oxidase, with the putative transmembrane helices A and B indicated as well as the surface helix ab. The mature protein in *Arabidopsis* mitochondria begins at A14 [15]. The *Arabidopsis* alternative oxidase cDNA in plasmid pAtAOmKX (derived from pAOX) is truncated at the 5′ end, and begins with F13. The translation start of the protein in *E. coli* is believed to be at the first methionine (M25) following F13 [15]. The *Nco*I– *Kpn*I DNA fragment (lower box) subcloned into pNK allows mutagenesis of amino acids E83 through G221, and the *Kpn*I– *Afl*II DNA fragment (subcloned into pKA) from L223 through the end of the protein. The use of the *Kpn*I site for reinserting the mutagenized fragments into pAtAOmKX precludes the potential mutagenesis of Y222, and allows only some changes to the G221 and L223 codons.

The cloning vectors p8ANBN and p9ANBN were constructed from pUC118 and pUC119, respectively, by ligating the two complimentary oligonucleotides ANBN1 (ttaagccatggtgatcagctagcctgca) and ANBN2 (ggctagctgatcaccatggc) to the *Pst*I–*Kpn*I digested vectors. This yielded four new cloning sites: *Afl*II, *Nco*I, *Bcl*I, and *Nhe*I. The 425 bp *Nco*I–*Kpn*I fragment of pAtAOmKX was cloned into p8ANBN to form pNK and the 342 bp *Kpn*I–*Afl*II fragment of pAtAOmKX was cloned into p9ANBN to form pKA (Fig. 1). Each fragment was placed in the noncoding direction of *lacZ* to minimize the possibility of selection against the fragment. Random mutations were incorporated into the two fragments by error-prone PCR utilizing dITP [19] using the primers UNIV2 (acgacgttgtaaaacgacgg) and REV2 (tttcacacaggaaacagctatg), which anneal to pNK and pKA outside the cloned fragment. Sequence analysis indicated that these conditions resulted in a misincorporation rate of about 1 per 250 base pairs DNA. Following amplification, PCR products were phenol extracted and digested with protease, followed by a second phenol extraction. The pNK-derived PCR product was cut with *Nco*I and *Kpn*I, gel-purified, and ligated to the *Nco*I–*Kpn*I digested pAtAOmKX. The pKA-derived PCR product was likewise restricted and cloned into *Kpn*I–*Afl*II digested pAtAOmKX. The ligation mixture was electroporated into *E. coli* SASX41B, which was then plated on LB containing ALA, methionine, and ampicillin. After overnight incubation, colonies from these plates were combined to inoculate M63 + SG liquid medium containing ALA, methionine and ampicillin. The cells were grown to a density of 50 Klett units, diluted in M63 + SG with ampicillin, and spread on GA plates with 0.3 mM SHAM. These plates were incubated for 3 days at 37°C to select for resistant colonies.

DNA was sequenced using Sequenase2 (Amersham, Arlington Heights, IL) and a modified protocol to eliminate artifact banding [20]. DNA was prepared by standard miniprep procedures or column purification (Qiagen, Chatsworth, CA).

2.3. Isolation of membranes

For assay of alternative oxidase activity, a single colony of *E. coli* SASX41B freshly transformed with the desired plasmid on LB plates containing ALA, methionine, and ampicillin was used to inoculate 25 ml of M63 + SG with ampicillin, ALA, and methionine. This preculture was grown for 4–5 h at 37°C with shaking to a mid-log density of 30–80 Klett units. The cells were then pelleted ($1100 \times g$, 10 min), the residual medium removed, and resuspended in 10 ml M63 + SG with ampicillin and methionine. A 2–5-ml aliquot of this suspension was used to inoculate 350 ml of the same medium for overnight growth at 37°C.

The *E. coli* cells were harvested and suspended in 50 mM KPi buffer, pH 7.0 containing 0.5 mM PMSF and 10 ug/ml each RNase and DNase, and disrupted by one pass through a French Press at 18 000 psi. The unbroken cells were removed ($3000 \times g$, 10 min) and the supernatant was centrifuged at $200\,000 \times g$ for 1 h to isolate the membranes. The membrane pellet was homogenized in 1–2 ml of 15% sucrose, 50 mM potassium phosphate, 1 mM EDTA, including 10 mM pyruvate unless indicated.

2.4. Assay of activity and inhibitor titration

Alternative oxidase activity was assayed polarographically as SHAM-sensitive oxygen consumption at 25°C in reaction buffer containing 50 mM potassium phosphate, 10 mM KCl, 5 mM $MgCl_2$, 1 mM EDTA, and, unless noted otherwise, 5 mM pyruvate, pH 7.0, with 0.5 mM duroquinol. Duroquinol was dissolved in acidic nitrogen-purged DMSO, and the concentration was determined spectrophotometrically [21]. SHAM and propyl gallate (PG) were dissolved in nitrogen-purged DMSO, and the DMSO concentration was kept constant in the assay. For determination of the inhibitor concentration at half-maximal inhibition of activity (I_{50}), membranes were incubated for 1 min in the presence of the SHAM or PG prior to the addition of duroquinol. The I_{50} was obtained from a plot of percentage inhibition vs. LOG inhibitor concentration, fitting the data to a standard titration curve with a nonlinear curve-fitting algorithm using SigmaPlot software. Protein was determined using a modified Lowry method [22].

3. Results

3.1. Effect of alternative oxidase inhibitors on E. coli respiration

E. coli DH5α was grown overnight in LB and membranes were isolated as described in Section 2. The oxidation of duroquinol by the wild-type *E. coli* respiratory pathway was partially inhibited by the alternative oxidase inhibitor SHAM, although not by PG (Fig. 2A–B). Assay of membranes of *E. coli* GO103 (which lacks the cytochrome *bd* oxidase) also showed partial inhibition of the duroquinol oxidase activity by SHAM, and the lack of effect of PG, suggesting that the site of SHAM inhibition is the cytochrome *bo* oxidase (Fig. 2C–D). SHAM at 1 mM showed a 30% inhibition and 3 mM SHAM gave 54% inhibition of the cytochrome *bo* oxidase. (It was not investigated whether there was in addition an effect of SHAM on the cytochrome *bd* oxidase.) Overnight growth of *E. coli* SASX41B/pAtAOmKX

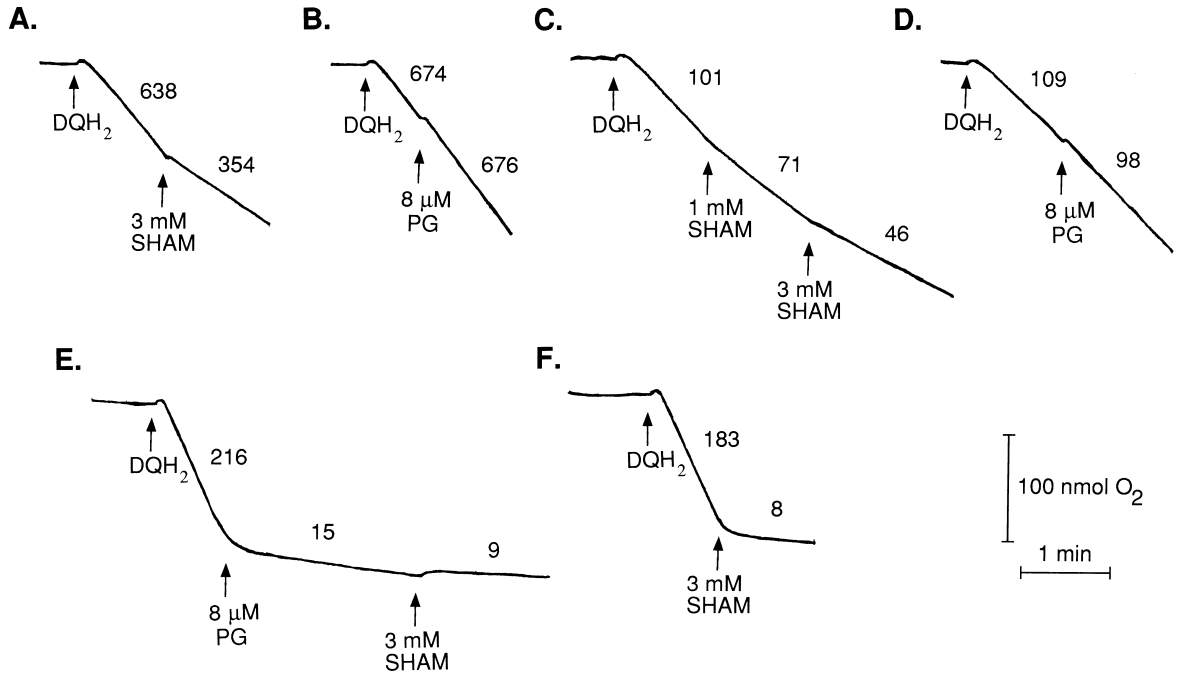

Fig. 2. Inhibition of oxygen consumption in isolated membranes of *E. coli*. Oxygen uptake was measured polarographically with duroquinol (DQH_2) as a substrate as described in Section 2. (A), (B) Membranes isolated from *E. coli* DH5α grown overnight in LB medium. (C), (D) Membranes isolated from *E. coli* GO103 grown overnight in LB medium with 25 μg/ml kanamycin. (E), (F) Membranes isolated from *E. coli* SASX41/pAtAOmKX grown in M63 + SG in the absence of ALA. Numbers next to the traces refer to oxygen consumption in nmol O_2 min^{-1} (mg protein)$^{-1}$.

in M63 + SG in the absence of ALA fully depletes the cytochrome *bo* oxidase, as seen in Fig. 2E. Here PG inhibits the alternative oxidase, leaving only a small residual oxygen uptake that is resistant to inhibition. Therefore, under these growth conditions, titration of duroquinol oxidase activity in *E. coli* SASX41B/pAtAOmKX with SHAM will accurately reflect an effect on the alternative oxidase without interference by the *E. coli* quinol oxidases (Fig. 2E).

3.2. Expression of the Arabidopsis alternative oxidase in E. coli SASX41B

Using membranes isolated and stored in the absence of pyruvate, the alternative oxidase was 50% activated at a concentration of 100 μM pyruvate. The I_{50} for SHAM was found to be independent of pyruvate with an I_{50} of 40 and 41 μM for membranes isolated in the absence and presence of 10 mM pyruvate, respectively. It was observed that when *E. coli* cells were broken in the absence of pyruvate and resuspended in buffer containing 10 mM pyruvate, that the activity of the enzyme would increase 180% over the course of 24 h storage on ice. For the same membranes resuspended without pyruvate and stored on ice, the remaining activity after 24 h had decreased to 70% of the initial activity. These measurements were made with 5 mM pyruvate present in the assay buffer. Subsequent to this observation, all membranes were isolated and resuspended in the presence of 10 mM pyruvate.

SHAM inhibited the *Arabidopsis* alternative oxidase in *E. coli* membranes with an average I_{50} of 42 μM (Table 1, line 1) while the I_{50} for PG was 390 nM. SHAM inhibited the alternative oxidase in a mixed competitive/noncompetitive fashion with respect to duroquinol, as seen in the Dixon plot shown in Fig. 3. The K_i and K_i' for inhibition were found to be 80 μM and 20 μM using the enzyme kinetics program LEONORA [23] to provide the best fit of the data.

3.3. Mutagenesis of the Arabidopsis alternative oxidase

Two fragments of the *Arabidopsis* alternative oxidase gene were subcloned for mutagenesis. The plasmid pNK contains the NcoI–KpnI fragment of the *Arabidopsis* alternative oxidase gene, encoding the central portion of the enzyme which includes one highly-conserved hydrophilic region surrounded by two putative hydrophobic transmembrane helices (Fig. 1). Plasmid pKA contains the C-terminal region of the alternative oxidase and includes the residues that have been postulated to ligate the iron center. The fragments were mutagenized by error prone PCR, recloned into pAtAOmKX, and SHAM-resistant colonies were selected as described in Section 2. A

Table 1
Resistance of alternative oxidase mutants to SHAM and PG

Mutation	Plasmid	I_{50} SHAM (μM)	Relative resistance, SHAM	I_{50} PG (nM)	Relative resistance, PG
none	AtAOmKX	42	(1.0)	390	(1.0)
F215L	NA11	69	1.6	360	0.9
M219I	NC6	57	1.4	420	1.1
M219V	NG1	73	1.7	390	1.0
	NT5				
	NT4				
	NA13				
	NA6				
G303E	KA2	194	4.6	440	1.1
	KA2b				
	KA13				

Membranes of *E. coli* SASX41B transformed with the indicated plasmid were isolated as described in Section 2. The concentration of SHAM and PG necessary for 50% inhibition of alternative oxidase activity (I_{50}) was determined. The relative resistance is expressed as the ratio of the I_{50} for the mutant to the I_{50} of the wild-type alternative oxidase.

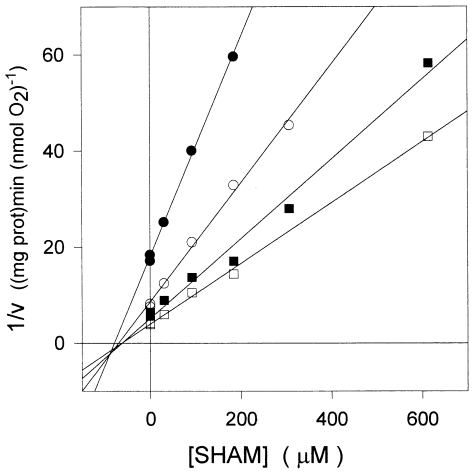

Fig. 3. Dixon plot of the SHAM inhibition of the *Arabidopsis* alternative oxidase activity expressed in *E. coli*. *E. coli* SASX41B/pAtAOmKX was grown in the absence of ALA and membranes were isolated as described in Section 2. Duroquinol concentrations are 160 μM, (●); 320 μM, (○); 490 μM, (■); and 730 μM (□).

few hundred SHAM-resistant colonies were isolated originating from twenty-four independent PCR reactions pooled for eight independent transformations. About 100 colonies were rescreened for SHAM resistance by isolating the plasmid, transforming fresh *E. coli* SASX41B, and replating the cells on selective medium.

The colonies chosen for further analysis were normal size (similar to *E. coli* SASX41B/pAtAOmKX) when growing on GA medium in the absence of SHAM, and larger than normal (i.e., resistant) in the presence of 0.3 mM SHAM. To verify the SHAM-resistant phenotype, membranes were isolated from *E. coli* SASX41B containing mutant plasmids grown as described in Section 2. Duroquinol oxidase activity was titrated with SHAM to determine the degree of resistance. The uninhibited duroquinol oxidase activity for the wild-type alternative oxidase (pAtAOmKX) ranged from 100 to 300 nmol O_2 min^{-1} mg $protein^{-1}$. The uninhibited activity for the mutant plasmids varied from 50 to 600 nmol O_2 min^{-1} mg $protein^{-1}$ and was probably a function of the level of inoculum and growth time, as there was no correlation with the mutation. Data from a representative experiment are shown in Fig. 4. A standard titration curve was fit to the data to determine the I_{50} for each plasmid, and the results for all the mutations are summarized in Table 1. Sequence analysis identified four mutations at three positions: F215L, M219I, M219V and G303E. The mutations found at residues F215 and M219 result in an alternative oxidase with only a slight resistance to SHAM of approximately 1.5-fold. The G303E mutation, in contrast, confers a 4.6-fold resistance to SHAM. None of the mutations have any effect on the resistance of the alternative oxidase to PG (Table 1).

Residues F215 and M219 are located in a region which is predicted by a Chou–Fasman algorithm [24] to have helical character (Fig. 5). These residues are in the vicinity of a highly conserved sequence beginning with G221 (GYLEEEA) (Fig. 6A). In contrast, G303E is three residues prior to the C-terminus of the

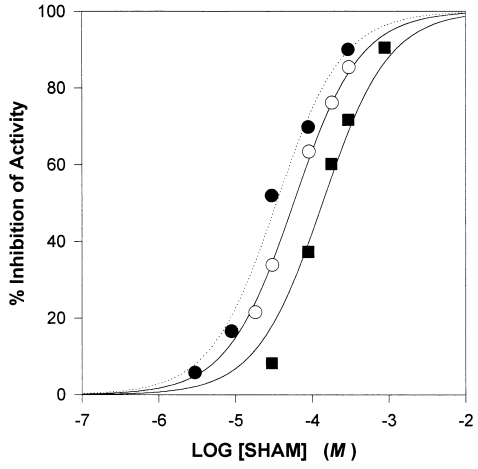

Fig. 4. A representative SHAM titration of alternative oxidase activity in isolated *E. coli* membranes. *E. coli* SASX41B with the indicated plasmid was grown in the absence of ALA and the membranes isolated as described in Section 2. SHAM was incubated with the membranes for 1 min at 25°C, at which point duroquinol was added to start the reaction. After about 1 min, 1 mM SHAM was added, and the resulting small level of residual activity was subtracted from the initial rate. To obtain '% inhibition' for each concentration of SHAM, the net rate was subtracted from the uninhibited net rate, and this value was divided by the uninhibited net rate. The data were fit with a standard titration curve. The wild-type alternative oxidase (●), expressed from pAtAOmKX, gave an I_{50} of 34 μM. The mutants M219I (pNC6) (○) and G303E (pKA2) (■) yielded an I_{50} of 57 μM and 136 μM, respectively. The uninhibited activity was 93, 625, and 110 nmol O_2 min^{-1} (mg protein)$^{-1}$ for wild type, M219I, and G303E.

enzyme in a relatively poorly conserved region of the protein (Fig. 5). Of the five M219V mutations isolated, four are known to be independently derived, as three independent pools of PCR reactions are involved (NA, NG, and NT) and the NA13 plasmid contains three silent mutations. The two G303E plasmids pKA2 and pKA13 may not be independent.

Because of the unexpected location of G303E, the small *Sty*I–*Afl*II fragment containing this mutation was recloned into pAtAOmKX. This construct, which has the last 15 amino acids of the alternative oxidase derived from pKA2, was named pKA2b. The I_{50} of the alternative oxidase expressed from pKA2b was similar to that of pKA2 and pKA13, verifying the source of the phenotype as G303E.

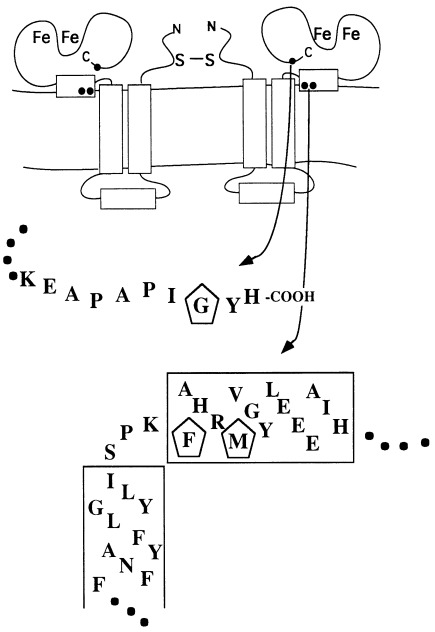

Fig. 5. A model of the *Arabidopsis* alternative oxidase (in its disulfide-bridged, inactive state) showing the position of the mutated residues. In the upper portion of the diagram, the amino terminus and the carboxy terminus are designated by 'N' and 'C,' respectively. F215, M219, and G303 are shown enclosed in pentagons. The C-terminal region must be located in proximity to the putative surface helix in order that G303, F215, and M219 can all interact with SHAM. In the text the helices are referred to as follows, observing the convention for membrane proteins: Starting at the N-terminus, the first transmembrane helix is designated 'helix A'; the intervening loop, helix ab; the second transmembrane helix, helix B; and the four helices of the proposed four-helix cluster, c, d, e, and f. (Of the latter four helices, only helix c is explicitly depicted here.)

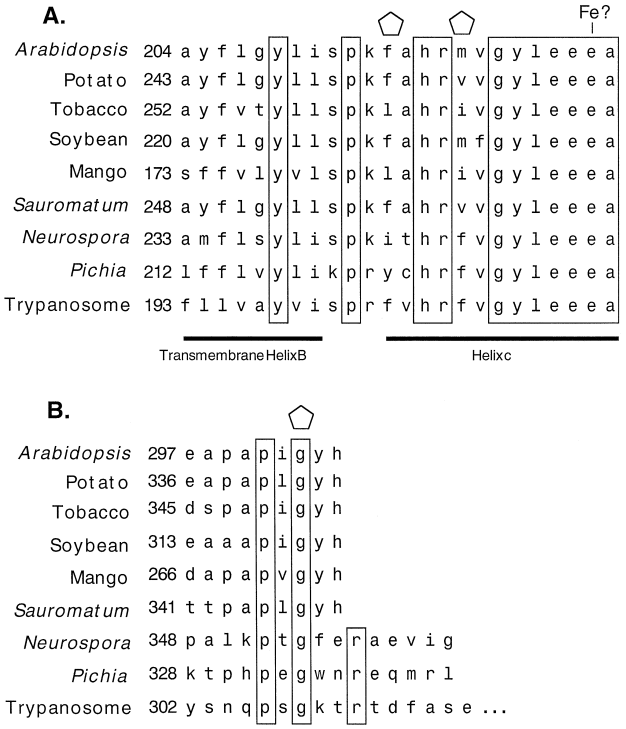

Fig. 6. Alignment of nine alternative oxidase sequences. Pentagons indicate residues found to confer inhibitor resistance when mutated. 'Fe?' indicates a potential iron ligand according to Moore et al. [5]. Boxed residues are conserved amino acids. (A) The alignment around F215 and M219. The residues comprising the c-terminal end of transmembrane helix B and those of putative surface helix c are underlined. (B) The C-terminal region of the alternative oxidase. Sequences are taken from *Arabidopsis* [15]; potato [25]; tobacco [26]; soybean [27]; mango [28]; *Sauromatum* [29]; *Neurospora* [30]; *Pichia* [31]; and trypanosome [32].

4. Discussion

4.1. Effect of SHAM and PG on E. coli respiration

Two commonly used inhibitors of the alternative oxidase, SHAM and PG, were tested for their effect on *E. coli* respiration. PG did not inhibit wild-type *E. coli* respiration. However, it was found that 1 mM SHAM inhibited the cytochrome *bo* oxidase by 30% (Fig. 2C). A previous report noted that 200 μM SHAM did not inhibit the cytochrome *bo* oxidase

[33], and this result is consistent with the high concentration of SHAM (3 mM) needed to obtain 50% inhibition. Until now sensitivity to SHAM coupled with resistance to cyanide has been considered to be the functional definition of a plant-type ubiquinol:oxygen oxidoreductase [34]. It is interesting to note that the cyanide-sensitive, heme-containing cytochrome *bo* oxidase can be sensitive to SHAM, albeit at high concentration. SHAM can no longer be regarded as a inhibitor specific to plant-type ubiquinol oxidases when working with prokaryotic systems. In the current work, PG-inhibition of the alternative oxidase was used to verify that the isolated membranes were devoid of duroquinol oxidase activity owing to endogenous *E. coli* oxidases.

4.2. Characterization of the Arabidopsis alternative oxidase expressed in E. coli

A direct comparison of the properties of the *Arabidopsis* alternative oxidase in isolated *E. coli* membranes to that found in *Arabidopsis* mitochondria is not available because of the limited use of *Arabidopsis* for mitochondrial studies. However, the alternative oxidase expressed in *E. coli* was found to similar to the alternative oxidase found in other plant mitochondria. The rate of oxygen consumption seen in wild type and mutants ranged from 50–600 nmol O_2 min^{-1} (mg protein)$^{-1}$; the low rate can be considered typical for nonaroid mitochondria, whereas the high value can often be observed in mitochondria isolated from aroid spadix tissue. A more rigorous comparison of activity by turnover number is not possible at this point because of the lack of a spectral feature with which to quantify the enzyme in either mitochondria or *E. coli* membranes. The alternative oxidase in isolated *E. coli* membranes was activated half-maximally with 100 μM pyruvate. This is similar to the values of 100 μM and 500 μM observed in soybean root [35] and tobacco leaf mitochondria [36], respectively. In contrast, with inside-out submitochondrial particles of sweet potato or soybean cotyledon, half-maximal activation was observed with a concentration of pyruvate as low as 5 μM [37].

The I_{50} for the inhibition of the alternative oxidase activity in *E. coli* SASX41B/pAtAOmKX membranes with SHAM was 40 μM, which is similar to that found in mung bean hypocotyl mitochondria (60 μM) but low relative to aroid (skunk cabbage) spadix mitochondria (260 μM) [38]. Using a Dixon plot, the inhibition was found to be mixed competitive/noncompetitive with respect to duroquinol, with a K_i and K_i' of 20 μM and 80 μM. In aroid (*Arum maculatum*) mitochondria, mixed competitive/noncompetitive inhibition was previously observed, with inhibition constants of 53 and 490 μM for SHAM, and for the more hydrophobic *m*-chlorohydroxamic acid, 25 μM and 81 μM [39]. For the other commonly used inhibitor of the alternative oxidase, PG, the I_{50} for the *Arabidopsis* enzyme in *E. coli* is 390 nM, significantly lower than that reported for mung bean mitochondria (3–4 μM) [40].

4.3. Recovery of inhibitor-resistant mutants of the alternative oxidase

Mutation of three amino acids, F215, M219, and G303 in the *Arabidopsis* alternative oxidase each led to a phenotype of increased SHAM-resistance when the protein was expressed in the heme-deficient strain *E. coli* SASX41B. Each of the three mutations of Phe and Met (F215L, M219V, and M219I) is conservative, maintaining the relative hydrophobicity of the original amino acid. Upon titration of the isolated membranes, only a 1.5-fold increase in resistance to SHAM was found, and normal levels of alternative oxidase activity are present. In contrast, mutation of Gly to Glu near the C-terminus of the alternative oxidase gives a 4.6-fold resistance to SHAM. This residue is found in a poorly conserved region of the oxidase, and the mutation to Glu presents a dramatic change from the smallest amino acid to one with a large negatively-charged side chain. None of the SHAM-resistant mutations yielded any change in sensitivity of the alternative oxidase to PG.

Quinone-site inhibitor-resistance mutations recovered in other electron-transfer complexes are typically many times more resistant than the F215 and M219 alternative oxidase mutants reported here. Although the approximately 1.5-fold resistance obtained is small, it is readily distinguished from the wild-type level on a titration plot (Fig. 4), and it falls outside of the level of noise in the measurements (compare PG values in Table 1, which likely represent scatter). In

addition, the selection of five independently derived M219V mutations, as well as three different mutations within a four amino acid segment, argues for the importance of this region of the protein in modulating SHAM-binding. This approximately 50% increase in SHAM resistance for mutations at F215 and M219 of the *Arabidopsis* enzyme falls well within the species-to-species variation in SHAM resistance for the alternative oxidase as noted above [38]. And, this variability in resistance among species is consistent with the variability (with conservation of hydrophobic character) at positions which align to F215 and M219 among the known derived amino acid sequences (see discussion below). Although a 1.5-fold increase in resistance to SHAM may seem rather minimal, the change in ΔG between wild type and mutant for the binding of SHAM is sufficient to account for the loss of two van der Waal interactions, following the calculations of Link et al. [41].

It should also be noted that the selection protocol used here was particularly favorable towards recovery of mutants with a low level of resistance to SHAM. The concentration of SHAM that was used for selection allowed growth of *E. coli* expressing wild-type alternative oxidase within 1–2 additional days after the normal selection period of three days. Because of this low level of toxicity, colonies that were only slightly larger than the wild-type control were readily identified. Furthermore, a selection for higher resistance to SHAM appeared not to be possible because of the deleterious effect of high SHAM concentrations on aerobic growth of *E. coli* utilizing its endogenous terminal oxidases. This was attributed to chelation of iron in the growth medium by SHAM, as it was partially relieved by supplemental iron. However, it may also have involved an effect of SHAM on the cytochrome *bo* oxidase, although this was not investigated further.

4.4. Implications for the structure of the alternative oxidase

The amino acids F215 and M219 are four residues apart, and only a few residues away from the putative transmembrane helix B (Fig. 5). Neither residue is strictly conserved through the known alternative oxidase sequences, but as with the recovered mutations, the changes in each case preserve the hydrophobicity of each position (Fig. 6A). In mango and tobacco, F215 is replaced by Leu, in *Neurospora*, by Ile, and in *Pichia*, it is replaced by Tyr. In soybean, M219 remains the same, but in the other species it is replaced by Val (potato, *Sauromatum*), Ile (mango, tobacco), or Phe (*Neurospora*, *Pichia*, trypanosome) (Fig. 6A). Analysis of this region of the *Arabidopsis* alternative oxidase by a modified Chou–Fasman algorithm predicts helical character. An α-helical structure would place F215 and M219 on the same side of the helix, and likely oriented towards the membrane phase given their hydrophobicity (Fig. 5). Such a structure—a transmembrane helix followed by a surface helix—is a feature that is well represented among known and predicted quinone binding sites [11,12,42,43]. In addition, the C-terminal end of this putative surface helix c has been previously hypothesized on the basis of the E-X-X-H sequence motif to be part of a four-helix bundle that binds the metal center [5]. This places F215 and M219 in close proximity to the postulated binuclear iron center of the alternative oxidase.

Although G303 has not been previously reported as a conserved residue in the alternative oxidase, it is possible to align the nine sequences in Fig. 6B such that G303 and P301 are conserved throughout. In the case of the plant alternative oxidases, the conserved Gly and Pro are the third and fifth residues from the C-terminus; for the fungal sequences, they are the ninth and eleventh from the end. In the trypanosome alternative oxidase, the Gly and Pro are well within the sequence. A conserved Arg found three residues past the conserved Gly for the fungal and trypanosome sequences adds credibility to this alignment (Fig. 6B).

The identification of distant residues involved in SHAM resistance puts a constraint on the possible three-dimensional structure of the alternative oxidase. The relatively poorly-conserved C-terminal region must be located in spatial proximity to the putative surface helix c in order for G303 to interact with F215 and M219 (Fig. 5). The conserved residues P301 and G303 may play an important role at the active site of the alternative oxidase. Amino acids F215, M219, and G303 as well as neighboring conserved residues are good candidates for future study by site-directed mutagenesis.

Acknowledgements

This work was supported by USDA National Research Initiative Competitive Grant #94-37306-0736. I would like to thank Drs. M. Kumar and D. Söll for pAOX and *E. coli* SASX41B, Dr. R. Gennis for *E. coli* GO103, and Dr. G. Cecchini for helpful comments. Special thanks are due to Dr. R. Malkin who provided laboratory space and many useful discussions during the course of this work.

References

[1] G.C. Vanlerberghe, L. McIntosh, Alternative oxidase: from gene to function, Annu. Rev. Plant Physiol. Plant Mol. Biol. 48 (1997) 703–734.
[2] J.N. Siedow, A.L. Umbach, Plant mitochondrial electron transfer and molecular biology, Plant Cell 7 (1995) 821–831.
[3] D.A. Day, J.T. Wiskich, Regulation of alternative oxidase activity in higher plants, J. Bioenerg. Biomemb. 27 (1995) 379–385.
[4] D.A. Day, J. Whelan, A.H. Millar, J.N. Siedow, J.T. Wiskich, Regulation of the alternative oxidase in plants and fungi, Aust. J. Plant Physiol. 22 (1995) 497–509.
[5] A.L. Moore, A.L. Umbach, J.N. Siedow, Structure–function relationships of the alternative oxidase of plant mitochondria: A model of the active site, J. Bioenerg. Biomemb. 27 (1995) 367–377.
[6] D.A. Berthold, J.N. Siedow, Partial purification of the cyanide-resistant alternative oxidase of skunk cabbage (*Symplocarpus foetidus*) mitochondria, Plant Physiol. 101 (1993) 113–119.
[7] N. Minagawa, S. Sakajo, T. Komiyama, A. Yoshimoto, Essential role of ferrous iron in cyanide-resistant respiration in *Hansenula anomala*, FEBS Lett. 267 (1990) 114–116.
[8] J.N. Siedow, A.L. Umbach, A.L. Moore, The active site of the cyanide-resistant oxidase from plant mitochondria contains a binuclear iron center, FEBS Lett. 362 (1995) 10–14.
[9] J. Whelan, M. Hugosson, E. Glaser, D.A. Day, Studies on the import and processing of the alternative oxidase precursor by isolated soybean mitochondria, Plant Mol. Biol. 27 (1995) 769–778.
[10] A.L. Umbach, J.N. Siedow, The reaction of the soybean cotyledon mitochondrial cyanide-resistant oxidase with sulfhydryl reagents suggests that alpha-keto acid activation involves the formation of a thiohemiacetal, J. Biol. Chem. 271 (1996) 25019–25026.
[11] J.P. Allen, G. Feher, T.O. Yeates, H. Komiya, D.C. Rees, Structure of the reaction center from *Rhodobacter sphaeroides* R-26: Protein-cofactor (quinones and Fe^{2+}) interactions, Proc. Natl. Acad. Sci. U.S.A. 85 (1988) 8487–8491.
[12] J. Deisenhofer, H. Michel, The photosynthetic reaction center from the purple bacterium *Rhodopseudomonas viridis*, Science 245 (1989) 1463–1473.
[13] A. Trebst, The topology of the plastoquinone and herbicide binding peptides of photosystem II in the thylakoid membrane, Z. Naturforsch. C 41 (1986) 240–245.
[14] A.M. Colson, Random mutant generation and its utility in uncovering structural and functional features of cytochrome *b* in *Saccharomyces cerevisiae*, J. Bioenerg. Biomemb. 25 (1993) 211–220.
[15] A.M. Kumar, D. Söll, *Arabidopsis* alternative oxidase sustains *Escherichia coli* respiration, Proc. Natl. Acad. Sci. U.S.A. 89 (1992) 10842–10846.
[16] Y.J. Avissar, S.I. Beale, Identification of the enzymatic basis for δ-aminolevulinic acid auxotrophy in a *hemA* mutant of *Escherichia coli*, J. Bacteriol. 171 (1989) 2919–2924.
[17] A. Sasarman, M. Surdeanu, G. Szegli, T. Horodniceanu, V. Greceanu, A. Dumitrescu, Hemin-deficient mutants of *Escherichia coli* K-12, J. Bacteriol. 96 (1968) 570–572.
[18] T.J. Silhavy, M.L. Berman, L.W. Enquist, Experiments with Gene Fusions, Cold Spring Harbor Laboratory Press, New York, 1984.
[19] J.H. Spee, W.M. de Vos, O.P. Kuipers, Efficient random mutagenesis method with adjustable mutation frequency by use of PCR and dITP, Nucleic Acids Res. 21 (1993) 777–778.
[20] M.S. Redston, S.E. Kern, Klenow cosequencing. A method for eliminating 'stops', Biotechniques 17 (1994) 286–288.
[21] R.R. Wise, A.W. Naylor, Calibration and use of a Clark-type oxygen electrode from 5 to 45°C, Anal. Biochem. 146 (1985) 260–264.
[22] G.L. Peterson, A simplification of the protein assay method of Lowry et al. which is more generally applicable, Anal. Biochem. 83 (1977) 346–356.
[23] A. Cornish-Bowden, Analysis of Enzyme Kinetic Data, Oxford Univ. Press, Oxford, 1995.
[24] P. Prevelige, Jr., G.D. Fasman, Chou–Fasman prediction of the secondary structure of proteins, in: G.D. Fasman (Ed.), Prediction of protein structure and the principles of protein conformation, Plenum, New York, 1989, pp. 391–416.
[25] C. Hiser, P. Kapranov, L. McIntosh, Genetic modification of respiratory capacity in potato, Plant Physiol. 110 (1996) 277–286.
[26] G.C. Vanlerberghe, L. McIntosh, Mitochondrial electron transport regulation of nuclear gene expression. Studies with the alternative oxidase of tobacco, Plant Physiol. 105 (1994) 867–874.
[27] J. Whelan, A.H. Millar, D.A. Day, The alternative oxidase is encoded in a multigene family in soybean, Planta 198 (1996) 197–201.
[28] A. Cruz-Hernandez, M.A. Gomez-Lim, Alternative oxidase from mango (*Magifera indica* L.) is differentially regulated during fruit ripening, Planta 197 (1995) 569–576.
[29] D.M. Rhoads, L. McIntosh, Isolation and characterization of a complementary DNA clone encoding an alternative oxidase protein of *Sauromatum guttatum* (Schott), Proc. Natl. Acad. Sci. U.S.A. 88 (1991) 2122–2126.

[30] Q. Li, R.G. Ritzel, L.T. McLean, L. McIntosh, T. Ko, H. Bertrand, F.E. Nargang, Cloning and analysis of the alternative oxidase gene of *Neurospora crassa*, Genetics 142 (1996) 129–140.

[31] S. Sakajo, N. Minagawa, T. Komiyama, A. Yoshimoto, Molecular cloning of cDNA for antimycin A-inducible mRNA and its role in cyanide-resistant respiration in *Hansenula anomala*, Biochim. Biophys. Acta 1090 (1991) 102–108.

[32] M. Chaudhuri, G.C. Hill, Cloning, sequencing and functional activity of the *Trypanosoma brucei brucei* alternative oxidase, Mol. Biochem. Parasitol. 83 (1996) 125–129.

[33] B. Meunier, S.A. Madgwick, E. Reil, W. Oettmeier, P.R. Rich, New inhibitors of the quinol oxidation sites of bacterial cytochromes *bo* and *bd*, Biochemical 34 (1995) 1076–1083.

[34] J.N. Siedow, The nature of the cyanide-resistant pathway in plant mitochondria, Recent Adv. Phytochem. 16 (1982) 47–83.

[35] A.H. Millar, J.T. Wiskich, J. Whelan, D.A. Day, Organic acid activation of the alternative oxidase of plant mitochondria, FEBS Lett. 329 (1993) 259–262.

[36] G.C. Vanlerberghe, D.A. Day, J.T. Wiskich, A.E. Vanlerberghe, L. McIntosh, Alternative oxidase activity in tobacco leaf mitochondria. Dependence on tricarboxylic acid cycle-mediated redox regulation and pyruvate activation, Plant Physiol. 109 (1995) 353–361.

[37] A.H. Millar, M.H.N. Hoefnagel, D.A. Day, J.T. Wiskich, Specificity of the organic acid activation of alternative oxidase in plant mitochondria, Plant Physiol. 111 (1996) 613–618.

[38] G.R. Schonbaum, W.D. Bonner Jr., B.T. Storey, J.T. Bahr, Specific inhibition of the cyanide-insensitive respiratory pathway in plant mitochondria by hydroxamic acids, Plant Physiol. 47 (1971) 124–128.

[39] C.J. Kay, J.M. Palmer, Solubilization of the alternative oxidase of cuckoo-pint (*Arum maculatum*) mitochondria. Stimulation by high concentrations of ions and effects of specific inhibitors, Biochem. J. 228 (1985) 309–318.

[40] J.N. Siedow, M.E. Girvin, Alternative respiratory pathway. Its role in seed respiration and its inhibition by propyl gallate, Plant Physiol. 65 (1980) 669–674.

[41] T.A. Link, U. Haase, U. Brandt, G. von Jagow, What information do inhibitors provide about the structure of the hydoquinone oxidation site of ubihydroquinone:cytochrome *c* oxidoreductase?, J. Bioenerg. Biomemb. 25 (1993) 221–232.

[42] H. Michel, J. Deisenhofer, Relevance of the photosynthetic reaction center from purple bacteria to the structure of photosystem II, Biochemical 27 (1988) 1–7.

[43] G. Brasseur, A.S. Saribas, F. Daldal, A compilation of mutations located in the cytochrome *b* subunit of the bacterial and mitochondrial bc_1 complex, Biochim. Biophys. Acta 1275 (1996) 61–69.